3rd Spectral Line Shapes in Plasmas
Code Comparison Workshop

March 2–6, 2015

Marseille, France

Call for Submissions (rev. February 9, 2015)

Introduction

This document defines the particulars of the workshop submissions. In the sections below we define the case problems, the comparison quantities which we require and the detailed format of the data files that we will be expecting.

The webpage of the meeting is at http://plasma-gate.weizmann.ac.il/slsp3/. The submission files are to be uploaded to the same server using a web interface with userid and password. Details will be announced separately.

Timeline (2015):

January 5	—	web interface for file uploads opens
February 2	—	hotel booking deadline (the booking is via the registration website)
February 14	—	submission deadline
March 2	—	workshop opens
March 6	—	workshop adjourns

Contents

1 Statement of cases

We have selected a number of transitions to consider, given in Table 1. For each transition we are requesting results on a grid of electron densities (n_e) and temperatures ($T = T_\mathrm{e} = T_\mathrm{i}$). For each case, the atomic and plasma models are specified, and for some cases, there are more than one atomic or plasma model suggested. Unless specified otherwise, plasma is assumed quasi-neutral, consisting of electrons and a single type of ions.

Each calculation will be referenced by its subcase name. The subcase name is of the form Case_ID.N.T.M.F, where Case_ID is from the first column of Table 1, and the N, T, M, and F correspond, respectively, to the n_e, T, model, and external-field indices, each counting from 1. For example, 5.1.2.3.1 identifies H Lyman-α, calculated for $n_e = 10^{17}\,\mathrm{cm}^{-3}$ and $T = 10\,\mathrm{eV}$, assuming 8000 protons in a fixed volume as perturbers. Similarly, 8.2.1.1.3 stands for C VI Lyman-α in a plasma with $n_e = 4 \times 10^{21}\,\mathrm{cm}^{-3}$ and $T = 80\,\mathrm{eV}$ in the presence of a 3-kT magnetic field.

The models suggested are limited – some by design, others by necessity, to make them manageable without too much computational resources and human time spent. If you feel that the best suggested model for a particular case is still too far from reality, you are encouraged to submit a separate result using an alternative model you see fit best, using "0" as the model index. Submissions of all such results should include an adequate description of the model used in the `<comments>` field of the file (see Sec. 5).

2 Justification of cases and details

The first [1] and second ([2] and references therein) SLSP workshops were a great success. We have covered a lot of interesting and physically sound spectra lines in a variety of plasma conditions.

However, the spread of results for some of the cases has remained unexplained. Therefore, we decided this time to focus on the few most problematic issues but deepen the analysis by requesting more internal data (such as the unitarity checks) and/or explicitly specifying fine-grained conditions (e.g., accounting for only a subset of the Maxwellian population of perturbers). In a sense, we are entering the "debug" mode.

Following the SLSP2 example, we also continue with the "experimental" cases, suggesting to interpret real-life spectroscopic data.

2.1 Ion dynamics – slow/fast fields

We want to separate the effects on the line profiles of slow and high-velocity particles—those with velocity $v \le v_{1/2}$ and $v > v_{1/2}$, respectively. Here, $v_{1/2}$ is the median velocity, such that

$$\int_0^{v_{1/2}} f(v)dv = \int_{v_{1/2}}^{\infty} f(v)dv, \tag{1}$$

and amounts to $v_{1/2} \approx 1.538\sqrt{kT/m}$ (m is the reduced perturber mass for μ-models and like).

1. Hydrogen Lyman-α is the classical ion-dynamics test and yet it has proven to be the most problematic case (with the largest spread of results from different calculations) in the previous workshops.

2. Hydrogen Lyman-β. Similarly to the previous case, but now a line with no central component.

2.2 Ion dynamics – with pre-defined field histories

Here, we provide calculated microfield histories to be used by *all* codes; the idea is, evidently, to single out the cause of the spread between different codes in the resulting lineshapes. Of course, these cases are primarily intended for simulations, but some models may try to adapt by using the field properties (the statistical distribution etc). In addition to the lineshapes, we want to check for deviations from unitarity:

$$\epsilon_i(t) = \max|U(t)U^\dagger(t) - 1|, \tag{2}$$

where $U(t)$ is the time evolution operator, and by $|..|$ we define here the absolute value as applied to each element of the matrix expression, and then the maximal element is chosen. i is the run number ($i = 1..N_r$)

Table 1: Case definitions.

ID	Transition(s)	# of subcases	n_e (cm^{-3})	T (eV)	Extra parameters
1	H Lyman-α	$1 \times 3 \times 3 \times 1 = 9$	10^{18}	1, 10, 100	—
			Model: $\Delta n \neq 0$ interactions ignored (strictly linear Stark effect); no fine structure; OCP proton plasma (assume Debye screening by electrons but no electron broadening effects) in **three** variants: $v \leq v_{1/2}$, $v > v_{1/2}$, and total.		
2	H Lyman-β	$1 \times 3 \times 3 \times 1 = 9$	10^{17}	1, 10, 100	—
			Model: Same as above.		
3	H Lyman-α	$2 \times 2 \times 1 \times 1 = 4$	n_1, n_2	T_1, T_2	—
			Model: $\Delta n \neq 0$ interactions ignored (strictly linear Stark effect); no fine structure. The microfields are given.		
4	H Lyman-β	$2 \times 2 \times 1 \times 1 = 4$	n_1, n_2	T_1, T_2	—
			Model: Same as above.		
5	H Lyman-α	$1 \times 3 \times 7 \times 1 = 21$	10^{17}	1, 10, 100	—
			Model: $\Delta n \neq 0$ interactions ignored (strictly linear Stark effect); no fine structure; ideal OCP electron plasma (straight path trajectories and infinite Debye length). Assume a fixed plasma volume containing 125×8^k particles with $k = 0, 1, 2, 3, 4, 5, \infty$.		
6	Li I 2s–2p	$1 \times 6 \times 1 \times 1 = 6$	10^{17}	1, 2, 5, 10, 20, 50	—
			Model: 2s and 2p levels included, no fine structure. Only **fixed-energy** electron broadening is included. No Debye screening.		
7	B III 2s–2p	$1 \times 6 \times 1 \times 1 = 6$	10^{18}	4, 7, 10, 20, 50, 100	—
			Model: Same as above.		
8	C VI Lyman-α	$2 \times 1 \times 2 \times 4 = 16$	10^{21}, 4×10^{21}	80	0, 1, 3, 10 kT
			Model: $\Delta n \neq 0$ interactions ignored (strictly linear Stark effect) in **two** variants: without and with fine structure; carbon plasma at LTE.		
9	Ar XVIII Lyman-α	$1 \times 1 \times 2 \times 4 = 8$	10^{22}	1000	$I = 10^{19}\,\mathrm{W/cm^2}$, $\omega = 2 \times 10^{15}\,\mathrm{rad/s}$
			Model: $\Delta n \neq 0$ interactions ignored in **two** variants: without and with fine structure; argon plasma at LTE. The laser fields included in **four** configurations: no field at all, only F, only B, and $F \times B$.		
10	H $n = * \to 1$	$3 \times 1 \times 2 \times 1 = 6$	10^{15}, 10^{16}, 10^{17}	1	—
			Model: fully ionized H plasma, **two** variants: only bound-bound transitions included or both bound-bound and free-bound.		
11	He II Paschen-α	$2 \times 2 \times 2 \times 1 = 8$	10^{18}, 10^{19}	4, 10	—
			Model: without and with $\Delta n \neq 0$ couplings accounted for; helium plasma under LTE.		
11a	He II Paschen-α	1	*	*	*
11b	He II Paschen-α	1	*	*	*
11c	He II Paschen-α	1	*	*	*
11d	He II Paschen-α	1	*	*	*
			Model: Do your best!		
12	H Balmer-α	$2 \times 2 \times 1 \times 1 = 4$	10^{16}, 10^{17}	0.5, 2	—
			Model: ions: protons.		
12a	H Balmer-α	1	*	*	*
12b	H Balmer-α	1	*	*	*
12c	H Balmer-α	1	*	*	*
12d	H Balmer-α	1	*	*	*
			Model: Do your best!		

The following entities are required:

$$E(t) = \frac{1}{N_r} \sum_{i=1}^{N_r} \epsilon_i(t) \tag{3}$$

and

$$E_m = \max_{i,t} \epsilon_i(t). \tag{4}$$

$E(t)$ should be provided on a grid of at least 100 points spanning from $t = 0$ to $t = t_1$, where t_1 is the time duration of a single run.

Similar to the previous case, Lyman-α and Lyman-β will be analyzed.

3. Hydrogen Lyman-α;
4. Hydrogen Lyman-β.

Please refer to Sec. 4 for a download link and detailed description of the field history file.

2.3 Convergence of line broadening in ideal plasma model

These cases are inspired by a recent study [3] suggesting the ideal plasma model (*non*-interacting Coulomb perturbers) imposes need to use a huge number of particles to achieve a proper convergence in the line width. To this end, we ask to make calculations assuming a series of spherical plasma volumes with progressively increasing radii R_k and respectively increasing number of contained perturbers (electrons) $N_k = 125 \times 8^k$, with $k = 0, 1, 2, 3, 4, 5, \infty$. If such a sharp cut-off is impossible within your model, please assume the usual Debye shielding with $\lambda_D = R_k$.

5. Hydrogen Lyman-α. The atomic model is the simplest one: a pure linear Stark effect (interactions between states with $\Delta n \neq 0$ ignored and no fine structure).

2.4 Isolated lines

$\Delta n = 0$ transitions in Li-like species present a puzzle by disagreement between experimental and different theoretical calculations [4]. For the first SLSP meeting, the Li-like 3s–3p isoelectronic sequence was considered, while for the second one, the 2s–2p resonance lines of the same sequence were calculated. We now continue with a deeper analysis of the 2s–2p series, asking, for the first time, to provide partial inelastic cross-sections.

For semiclassical models and simulations, these are to be calculated in the following way: The Lth partial wave contribution to the cross-section of transition from level i to level f is, for a given energy E,

$$\sigma_{if}^{(L)}(E) = \frac{2\pi}{g_i} \int_{R_{min}^{(L)}}^{R_{max}^{(L)}} \rho d\rho \sum_{m_i, m_f} |\langle J_i m_i | T(\rho, E) | J_f m_f \rangle|^2, \tag{5}$$

where g_i is the initial level degeneracy. T may be the S-matrix since the states are different and a square is taken. Different choices of R_{max} and R_{min} are discussed in [5]. The simplest one that we adopt here is

$$R_{min}^{(L)} = L \frac{\hbar}{mv}, \tag{6}$$

$$R_{max}^{(L)} = (L+1) \frac{\hbar}{mv}, \tag{7}$$

where $v = \sqrt{2E/m}$.

These $\sigma_{if}^{(L)}(E)$ should be provided at least for Ls from 0 to 10 (please go up to 100, if possible).

Only the dipole interactions should be accounted for. Each of the two species (below) is asked to be calculated for a single representative density. The plasma model for these cases consists only of electrons. Contrary to all other cases, here the electrons should be assumed to have a fixed energy (i.e., **not** a Maxwellian distribution). The width and shift (which are required, too) should also be calculated for the same fixed energy of the electrons. The energy values are listed in the "T" column of Table 1. Please also ignore the Debye screening, but if this is problematic for your calculations, assume screening corresponding to $T_e = E$.

6. Li I - the first, neutral, species in the sequence;

7. B III - one that ignited a long discussion some time ago [6].

2.5 External fields

8. C VI Lyman-α in the presence of strong external static magnetic field. The plasma parameters and fields are roughly similar to those found in laser-driven capacitor-coil target experiments [7]. The magnetic field is assumed to be parallel to the z axis.

9. Ar XVIII Lyman-α under external electromagnetic harmonic perturbation, e.g., a laser. The functional dependence of the electric and magnetic fields is $F\cos(\omega t)$ and $B\cos(\omega t)$, respectively ($\vec{F} \perp \vec{B}$), with ω and laser intensity given in Table 1 ($I = 10^{19}\,\mathrm{W/cm^2}$ approximately corresponds to the electric and magnetic field amplitudes of $8.66 \times 10^4\,\mathrm{MV/cm}$ and $2.89 \times 10^4\,\mathrm{T}$, respectively). The electric field is assumed to be parallel to the z axis, while the magnetic field—parallel to the x axis. Two variants of the atomic model: without and with the fine structure taken into account.

2.6 Ionization potential depression

Similar to case 12 from SLSP1, but for the Lyman series. Spectroscopy-wise, discrete transitions start to overlap between themselves and the free-bound continuum. A broad spectral region will be analyzed covering both discrete and continuum spectrum and a transition region in between.

10. H Lyman series at $T = 1\,\mathrm{eV}$ and three densities from 10^{15} to $10^{17}\,\mathrm{cm^{-3}}$. Please do **not** include the trivial $\exp(-\hbar\omega/T)$ factor in the spectrum output. The suggested spectral range (see Table 6) for this case covers transitions from Lyman-γ to continuum.

2.7 Modeling experimental data

A "real life" type of calculations. The objective of these cases is to discuss in detail how different researchers approach analysis of experimental spectra. To have a better understanding of why different approaches might end up with different best-fit plasma parameters, we also ask to calculate the relevant line shapes on a small predefined grid of parameters.

For these calculations (on the predefined grid), please submit only the Stark-broadened profiles, i.e., no Doppler broadening etc, while in the "best-fit" subcases (11a–d, 12a–d), include any relevant effects. Please note that the experimental data are unpublished, and are provided solely for the purpose of this workshop. For any other use, please contact the authors (see below) directly.

11. Hydrogen-like He II $n = 4 \to n = 3$ (Paschen-α) transition. We ask to calculate this case using two atomic models: without and with $\Delta n \neq 0$ couplings accounted for.

    The experimental data are time- and space-integrated. The challenge is to infer the plasma parameter distributions along the line of sight.

    Description of the experimental setup: exp_HeII.pdf

    Experimental spectrum at y = 1 mm (case 11a): exp_HeIIa.dat

    Experimental spectrum at y = 0.4 mm (case 11b): exp_HeIIb.dat

    Experimental spectrum at y = 0.2 mm (case 11c): exp_HeIIc.dat

    Experimental spectrum at y = 0 mm (case 11d): exp_HeIId.dat

    Units: $\mathrm{cm^{-1}}$.

12. Hydrogen Balmer-α is probably the most frequently calculated and measured line in the Stark broadening studies. In the experiment, the plasma densities inferred from the line profiles significantly (up to $\approx 40\%$) differ from the Thomson scattering data. It would be interesting to see whether with other calculations the discrepancies can be minimized or explained.

Description of the experimental setup: exp_Ha.pdf

We provide four spectra acquired at different positions and delays, see Fig. 1. T_e in the regions I, II, III, and IV, as inferred from the Thomson scattering measurements, are 2.23, 2.32, 1.21, and 1.20 eV, respectively.

Experimental spectrum at region I (case 12a): exp_Haa.dat

Experimental spectrum at region II (case 12b): exp_Hab.dat

Experimental spectrum at region III (case 12c): exp_Hac.dat

Experimental spectrum at region IV (case 12d): exp_Had.dat

Units: cm^{-1}.

3 Atomic data

In all cases, we assume the dipole approximation both for the radiation ($E1$) and the perturbation due to the plasma micro-fields. The relevant matrix elements are

$$\langle \alpha j m | r_q | \alpha' j' m' \rangle = (-1)^{j-m} \begin{pmatrix} j & 1 & j' \\ -m & q & m' \end{pmatrix} (\alpha j | r | \alpha' j') \,. \tag{8}$$

The reduced radius-vector matrix elements $(\alpha j|r|\alpha' j')$, relevant for the cases considered, are given below.

3.1 Hydrogen-like

For hydrogen ($Z = 1$) and hydrogen-like cases, the data are to be calculated analytically. For cases where the fine structure is neglected, the binding energies to be assumed are (in atomic units $E_\mathrm{H} \approx 27.211\,\mathrm{eV}$, corresponding to $\approx 2.1947 \times 10^5\,\mathrm{cm}^{-1}$)

$$E_n^0 = -\frac{Z^2}{2n^2} \,. \tag{9}$$

When the fine structure is asked to be accounted for, the energies are

$$E_{nj} = E_n^0 - \frac{\alpha^2 Z^4}{2n^3} \left(\frac{1}{j+1/2} - \frac{3}{4n} \right) , \tag{10}$$

where $\alpha \approx 7.2974 \times 10^{-3}$ is the fine-structure constant.

Reduced matrix elements of radius-vector are

$$(n\ell|r|n'\ell') = Z^{-1} (-1)^{\ell+\ell_>} \sqrt{\ell_>} R_{n\ell}^{n'\ell'} \,, \tag{11}$$

where $\ell_> = \max(\ell, \ell')$ and

$$R_{n\ell}^{n\ell-1} = -\frac{3}{2} n \sqrt{n^2 - \ell^2} \tag{12}$$

for diagonal terms (e.g., Eq. (63.5) in [8], but notice the wrong sign there!) and

$$R_{n\ell}^{n'\ell-1} = \frac{(-1)^{n'-\ell}}{4(2\ell-1)!} \sqrt{\frac{(n+\ell)!(n'+\ell-1)!}{(n-\ell-1)!(n'-\ell)!}} \frac{(4nn')^{\ell+1} (n-n')^{n+n'-2\ell-2}}{(n+n')^{n+n'}} \times$$
$$\left\{ F_{21}\left(-n_r, -n_r', 2\ell, -\frac{4nn'}{(n-n')^2} \right) - \left(\frac{n-n'}{n+n'} \right)^2 F_{21}\left(-n_r - 2, -n_r', 2\ell, -\frac{4nn'}{(n-n')^2} \right) \right\} \tag{13}$$

for off-diagonal ones (Eq. (63.2) in [8]). Here, F_{21} is the Gauss hypergeometric function and $n_r = n - \ell - 1$, $n_r' = n' - \ell$ are the radial quantum numbers of the two states. For convenience, the reduced matrix elements up to $n = 5$ are given in Table 2.

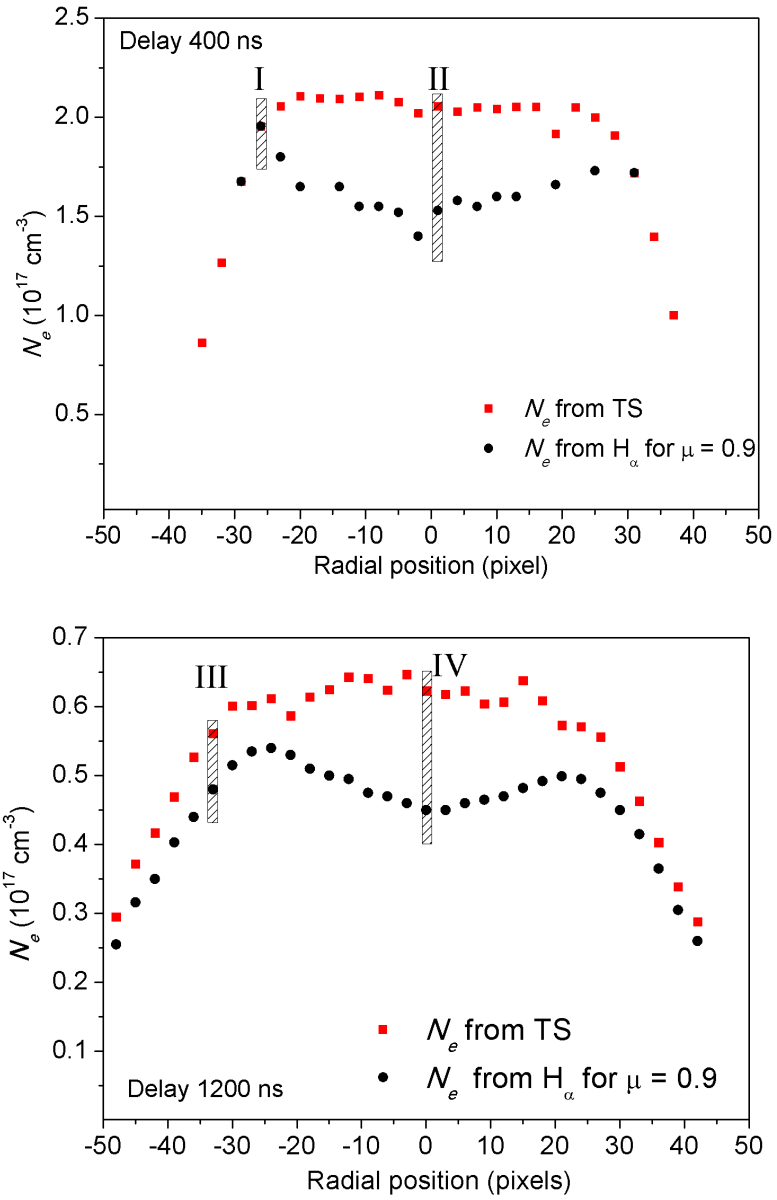

Figure 1: Four observation regions for the experimental spectra in case 12.

Table 2: Hydrogen reduced matrix elements up to $n = 5$.

	1s	2s	2p	3s	3p	3d	4s	4p	4d	4f	5s	5p	5d	5f
2p	-1.29	-5.20												
3s			0.938											
3p	-0.517	-3.06		-12.7										
3d			-6.71		-14.2									
4s			0.382		2.44									
4p	-0.305	-1.28		-5.47		1.84	-23.2							
4d			-2.418		-10.7			-29.4						
4f						-17.7			-27.5					
5s			0.228		0.970			4.60						
5p	-0.209	-0.774		-2.26		0.683	-8.52		4.31		-36.7			
5d			-1.38		-4.20			-15.6		2.88		-48.6		
5f						-5.75			-24.4				-52.0	
5g										-35.4				-45.0

Table 3: Atomic level energies for isolated lines.

Species	Level	Energy (cm^{-1})
Li I	2s	0.00
	2p	14903.89
B III	2s	0.00
	2p	48381.07

3.2 Non-hydrogen

The data are taken from the NIST on-line compilation [9]. The level energies, averaged over the fine-structure components for $\ell > 0$, are given in Table 3. The absolute values of the matrix elements are obtained from the respective multiplet-averaged absorption oscillator strengths f according to

$$|(n\ell|r|n'\ell')| = \sqrt{\frac{3f(2\ell'+1)}{2(E_{n\ell} - E_{n'\ell'})}}\,, \tag{14}$$

and sign as in respective H-like from Eqs. (11 – 13). The data are summarized in Table 4.

Table 4: Oscillator strengths for isolated lines.

Species	Transition	f
Li I	2s — 2p	7.472e-1
B III	2s — 2p	3.629e-01

4 Field histories for cases 3 and 4

The field history file contains 50 field histories, each of length 1,000,000. The sampling is at a constant time step. The file is a binary `FORTRAN` unformatted output, containing a header record followed by 1,000,000 records of 50 3D vector data points. The header record lists the number of histories (50), number of records in each (1,000,000), the time step Δt (s) and the normalized field in the units of V/m.

The "base" microfield histories are given with $\Delta t = 10^{-16}$ s and $F_0 = 3.74172\times10^7$ V/m. Various subcases assume these Δt and F_0 scaled as

$$F_0' = SF_0, \tag{15}$$

$$\Delta t' = s\Delta t, \tag{16}$$

with S and s given in Table 5. The table also lists prescribed lengths (number of time steps, $N_t = t_1/\Delta t$) and number of runs for each subcase. Note that $N_t N_r = \mathrm{const}$, and is equal to the total length of the microfield histories (50,000,000).

Table 5: Run parameters for cases 3 and 4.

Subcase	S	s	N_t	N_r
3.1.1.1.1	1	1	100,000	500
3.1.2.1.1	1	0.5	200,000	250
3.2.1.1.1	4	0.5	100,000	500
3.2.2.1.1	4	0.25	100,000	500
4.1.1.1.1	1	1	25,000	2,000
4.1.2.1.1	1	0.5	50,000	1,000
4.2.1.1.1	4	0.5	25,000	2,000
4.2.2.1.1	4	0.25	25,000	2,000

A sample `F77` file demonstrating reading in the data and writing them to *stdout* in the ASCII format is given in Listing 1; use it as a starting point. Please note that the binary data files are stored in the little-endian format, thus on big-endian machines one may need to explicitly specify data conversion, e.g., compile with ``gfortran -fconvert=little-endian''.

Run it, e.g., like

```
$ ./read_bin > fields.dat
 Enter file name:
fields.bin
 Histories =           50
    Length =      1000000
        dt =    1.00000002E-16
        F0 =    37417160.0
 Enter history #:
1
$
```

in order to get the first one million field data. The "fields.dat" file should be then

```
  0.1790E+01   0.4998E+00   0.2078E+00
  0.1789E+01   0.5005E+00   0.2078E+00
  0.1788E+01   0.5012E+00   0.2324E+00
  ...
```

5 Submission format

We use an XML-based format for submissions, with an example shown schematically in Listing 2.

Everything is included between the `<slsp>` and `</slsp>` tags. The meaning of other tags is described below:

`<case>` The subcase identification in the Case_ID.N.T.M.F format, see Sec. 1.

`<contributor>` The person who submits these results.

`<affiliation>` His/her affiliation.

`<code>` Name of the code/approach.

`<version>` Version of the code (optional).

`<date>` Date/time when the calculations were made.

`<comments>` Any comments you may like to make. The comments are optional, **except for advanced models (M=0 in the subcase id) and fitting experimental data (cases 11* and 12*)**. In the later cases, please describe the model employed with sufficient details. If the comments must contain "<" or "&" characters, enclose the entire text with "<![CDATA[" and "]]>":

Listing 1: An example program demonstrating reading in the binary field history files.

```
!     An example program demonstrating reading in the binary field
!     history files.

      program read_bin

      implicit none

      integer*4 j, l, nhistories, nrecords, iunit, ihist
      real*4 dt, F0, Fx, Fy, Fz
      character (20) f_name

      parameter(iunit = 1)

      write (0,*) 'Enter file name:'
      read (*, '(a)') f_name

      open (unit   = iunit,
     &      file   = f_name,
     &      form   = 'unformatted',
     &      status = 'old')

      read (iunit) nhistories, nrecords, dt, f0
      write (0,*) 'Histories = ', nhistories
      write (0,*) '   Length = ', nrecords
      write (0,*) '       dt = ', dt
      write (0,*) '       F0 = ', F0

      write (0,*) 'Enter history #:'
      read (*, '(i3)') ihist

      if (ihist .lt. 1 .or. ihist .gt. nhistories) then
          write (0,*) 'History # is out of range'
          stop
      end if

      do l = 1, nrecords
         read (iunit) (Fx, Fy, Fz, j = 1, ihist)
         write (6, '(3E12.4)') Fx, Fy, Fz
      end do

      close(iunit)

      end
```

Listing 2: An example of submission.

```
<?xml version="1.0"?>
<slsp>
  <case>1.1.1.3.1</case>
  <contributor>E. Stambulchik</contributor>
  <affiliation>WIS</affiliation>
  <code>simu</code>
  <version>1.9.0/1.4.0</version>
  <date>2011-12-13 18:34:39</date>

  <comments>
     These are my comments on this calculation.
  </comments>

  <time1>6.826e-11</time1>
  <nruns>400</nruns>

  <accuracy>-10 +5</accuracy>

  <field_distribution unit="128196">
    0.000000 0.000000
    0.025000 0.000421
    0.075000 0.002919
      ...
      ...
    29.875000 0.000333
    29.925000 0.000324
    29.975000 0.000316
  </field_distribution>

  <spectrum unit="1">
    -200.0 0.000741852
    -199.8 0.000751194
    -199.6 0.000747932
      ...
      ...
    199.6 0.000738701
    199.8 0.000752916
    200.0 0.000735306
  </spectrum>
</slsp>
```

```
<comments><![CDATA[
  Some bizarre & < > comments.
]]></comments>
```

<time1> Physical time (not CPU!), in seconds, the evolution of the atomic system is calculated for in a single run. (This and the following entry are specific for MD simulations. When irrelevant, skip or set to zero.)

<nruns> Number of runs used for averaging.

<accuracy> The estimated accuracy (in %) of the calculations, say of the FWHM. Only uncertainties introduced by the calculations should be included (in particular, not those due to an idealized/simplified plasma or atomic models suggested for this specific case). If the error bars are asymmetric, list two numbers with proper signs.

<spectrum> For all cases **except those concerned with isolated lines (6 – 7)**, we ask to provide entire line shapes on a reasonably dense grid, typically $\sim$ 1000 points (see Table 6). When the spectral range is symmetric ($\pm$ something), it means relative to the unperturbed position ω_0, calculated as a difference between the weighted-average energies of the initial and final levels:

$$\hbar\omega_0 = \frac{\sum_i g_i E_i}{\sum_i g_i} - \frac{\sum_f g_f E_f}{\sum_f g_f} \,. \tag{17}$$

The spectral windows and distances between the consecutive abscissas defined are recommended values. The relatively wide spectral windows are defined on purpose, to investigate far wings of the spectral lines. You can use denser and/or wider grids as you see fit. It is suggested to use equidistant grids. The units are cm^{-1}. The optional `unit` attribute allows for scaling the abscissas, e.g., by using `unit="8065.5"` one can output spectra in eV's. Where the spectra are requested and external fields specified (cases 8 and 9), the π ($\Delta M = 0$) and σ ($\Delta M = \pm 1$) polarizations will be needed separately (to be provided as the second and third columns, respectively):

```
...
...
<spectrum>
  w_1 I_pi(w_1) I_sigma(w_1)
  w_2 I_pi(w_2) I_sigma(w_2)
  ...
  ...
  w_N I_pi(w_N) I_sigma(w_N)
</spectrum>
...
...
```

It is assumed that

$$I_{\mathrm{tot}}(\omega) = I_\pi(\omega) + 2I_\sigma(\omega) \,. \tag{18}$$

In all cases, no normalization condition is imposed, but do preserve correct ratio between I_π and I_σ.

<field_distribution> Quasi-static field distribution (normalized) used for the calculation (due to all plasma particles, but excluding external fields, if any). The fields are in V/cm. The optional `unit` attribute allows for scaling the field strength values conveniently, e.g., by setting it to the Holtsmark normal field strength F_0 one obtains the distribution of the reduced field strengths. The distributions should be calculated on an equidistant grid covering at least $0 - 10$ with a step not exceeding 0.1 (in units of F_0).

<width> FWHM, **for isolated lines only (cases 6 and 7)**. In units of cm^{-1}.

<shift> Shift, for the same cases. In units of cm^{-1}.

<partial_xs> Partial cross-sections; these are also specific to the 6 and 7 cases. The format is

Table 6: Recommended spectral grids.

Subcase	Spectral range (cm^{-1})	Step (cm^{-1})
1.*.*.*.*	± 1,000	1
2.*.*.*.*	± 1,000	2
3.1.*.*.*	± 500	3
3.2.*.*.*	± 2,000	6
4.1.*.*.*	± 3,000	13
4.2.*.*.*	± 10,000	27
5.1.1.*.*	± 100	0.4
5.1.2.*.*	± 50	0.2
5.1.3.*.*	± 25	0.1
8.1.*.*.*	± 10,000	50
8.2.*.*.*	± 20,000	50
9.*.*.*.*	± 1,000,000	500
10.*.*.*.*	100,000 – 110,000	5
11.1.*.*.*	± 1,000	5
11.2.*.*.*	± 5,000	25
12.1.*.*.*	± 100	0.25
12.2.*.*.*	± 400	1

```
...
...
<partial_xs>
  L_1 sigma_e(L_1) sigma_d(L_1)
  L_2 sigma_e(L_2) sigma_d(L_2)
  ...
  ...
  L_N sigma_e(L_N) sigma_d(L_N)
</partial_xs>
...
...
```

For each L, partial excitation and de-excitation (for the same *incident* energy) cross-sections should be listed in the second and third columns, respectively [see Eq. (5) for semiclassical calculations and simulations]. The units are cm^2.

`<nonunitarity>` Deviation from unitarity, **only for cases 3 and 4**, in the following form:

```
...
...
<nonunitarity max="E_m">
  t_1 E(t_1)
  t_2 E(t_2)
  ...
  ...
  t_N E(t_N)
</nonunitarity>
...
...
```

Here, "E_m" is defined by Eq. (4), and the "E" array—by Eq. (3).

References

[1] E. Stambulchik. Review of the 1st Spectral Line Shapes in Plasmas code comparison workshop. *High Energy Density Phys.*, 9(3):528–534, 2013. doi:10.1016/j.hedp.2013.05.003.

[2] E. Stambulchik, A. Calisti, H.-K. Chung, and M. Á González. Special issue on spectral line shapes in plasmas. *Atoms*, 2(3):378–381, August 2014. doi:10.3390/atoms2030378.

[3] J. Rosato, H. Capes, and R. Stamm. Ideal Coulomb plasma approximation in line shape models: Problematic issues. *Atoms*, 2(2):253–258, 2014. doi:10.3390/atoms2020253.

[4] H. R. Griem and Yu. V. Ralchenko. Electron collisional broadening of isolated lines from multiply-ionized atoms. *J. Quant. Spectr. Rad. Transfer*, 65(1-3):287–296, 2000. doi:10.1016/S0022-4073(99)00074-6.

[5] S. Alexiou, R. W. Lee, S. H. Glenzer, and J. I. Castor. Analysis of discrepancies between quantal and semiclassical calculations of electron impact broadening in plasmas. *J. Quant. Spectr. Rad. Transfer*, 65(1–3):15–22, 2000. doi:10.1016/S0022-4073(99)00051-5.

[6] H. R. Griem, Yu. V. Ralchenko, and I. Bray. Stark broadening of the B III $2s - 2p$ lines. *Phys. Rev. E*, 56(6):7186–7192, 1997. doi:10.1103/PhysRevE.56.7186.

[7] S. Fujioka, Z. Zhang, K. Ishihara, K. Shigemori, Y. Hironaka, T. Johzaki, A. Sunahara, N. Yamamoto, H. Nakashima, T. Watanabe, H. Shiraga, H. Nishimura, and H. Azechi. Kilotesla magnetic field due to a capacitor-coil target driven by high power laser. *Scientific Reports*, 3, 2013. doi:10.1038/srep01170.

[8] H. A. Bethe and E. E. Salpeter. *Quantum Mechanics of One- and Two-Electron Atoms*. Plenum, New York, 1977.

[9] NIST Atomic Spectra Database. http://www.nist.gov/pml/data/asd.cfm. URL: http://www.nist.gov/pml/data/asd.cfm.